Method for Accurate Determination of Dissociation Constants of Optical Ratiometric Systems: Chemical Probes, Genetically Encoded Sensors, and Interacting Molecules

ARTICLE *in* ANALYTICAL CHEMISTRY · NOVEMBER 2013

Impact Factor: 5.64 · DOI: 10.1021/ac402637h · Source: PubMed

4 AUTHORS, INCLUDING:

Adam Pomorski
University of Wroclaw
6 PUBLICATIONS **31** CITATIONS
SEE PROFILE

Tomasz Kochańczyk
University of Wroclaw
5 PUBLICATIONS **27** CITATIONS
SEE PROFILE

Artur Krężel
University of Wroclaw
58 PUBLICATIONS **1,856** CITATIONS
SEE PROFILE

analytical chemistry

Article

pubs.acs.org/ac

Method for Accurate Determination of Dissociation Constants of Optical Ratiometric Systems: Chemical Probes, Genetically Encoded Sensors, and Interacting Molecules

Adam Pomorski,[†] Tomasz Kochańczyk,[†] Anna Miłoch, and Artur Krężel*

Laboratory of Chemical Biology, Faculty of Biotechnology, University of Wrocław, Joliot-Curie 14a, 50-383 Wrocław, Poland

Supporting Information

ABSTRACT: Ratiometric chemical probes and genetically encoded sensors are of high interest for both analytical chemists and molecular biologists. Their high sensitivity toward the target ligand and ability to obtain quantitative results without a known sensor concentration have made them a very useful tool in both in vitro and in vivo assays. Although ratiometric sensors are widely used in many applications, their successful and accurate usage depends on how they are characterized in terms of sensing target molecules. The most important feature of probes and sensors besides their optical parameters is an affinity constant toward analyzed molecules. The literature shows that different analytical approaches are used to determine the stability constants, with the ratio approach being most popular. However, oversimplification and lack of attention to detail results in inaccurate determination of stability constants, which in turn affects the results obtained using these sensors. Here, we present a new method where ratio signal is calibrated for borderline values of intensities of both wavelengths, instead of borderline ratio values that generate errors in many studies. At the same time, the equation takes into account the cooperativity factor or fluorescence artifacts and therefore can be used to characterize systems with various stoichiometries and experimental conditions. Accurate determination of stability constants is demonstrated utilizing four known optical ratiometric probes and sensors, together with a discussion regarding other, currently used methods.

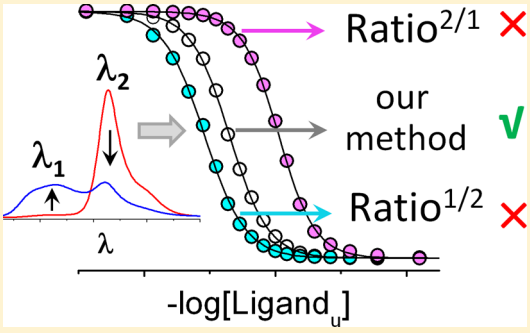

Optical probes are extremely useful tools in determination of the state and changes of physicochemical parameters of the environment where they are present. Optical changes are related to alterations in chromophore electronic state or conformational change of the sensing molecule upon binding of the target ligand such as a protein, ligand moiety, metal ion, or any other chemical agents. Calibration of the absorbance and fluorescence changes upon ligand binding allows one to determine the thermodynamic parameters associated with the changes, such as acidic dissociation constants, ligand binding constants and the cooperativity factor. The measurements based on the observation of intensity changes at single wavelength are frequently affected by a number of factors, especially when the probe is used in a heterogeneous environment (e.g., a cell), where autofluorescence tends to significantly affect the outcome of the experiment. The ratio of fluorescence or absorbance intensities at two suitably chosen wavelengths eliminates the differences in instrumental efficiency, environmental effects, and probe concentration and also offers a higher sensitivity. The milestone report by Grynkiewicz, Poenie, and Tsien in 1985 was instrumental in popularizing the usage of ratiometric probes and laid the basis for their internal calibration for both in vitro and in vivo conditions.[1,2] Currently, ratiometric probes, indicators, and genetically encoded protein sensors that are based on FRET or BRET are in the focus of interest in analytical chemistry as well as chemical and molecular biology. Examples include Ca(II) sensors GECO,[3] members of the Fura family[1] that rely on the ratiometric changes in fluorescence spectra, genetically encoded sensors based on FRET between two fluorescent proteins (eCALWY, FLIPE)[4,5] and BRET (pHlash).[6]

In early work, it was stated that determination of the apparent dissociation constant (K_d) of a sensor−ligand complex must be based on precisely processed experimental data in order to obtain proper values. These approaches generally accounted for 1:1 stoichiometries and various cooperativity.[1] Since that time, the experimental data processing and equations applied to calculate the K_d values seem to have been modified or simplified in various forms that clearly omit the fact that ratios of two different dynamic ranges of individual bands results in shifting the half-saturation point to other values of unbound (free) ligand (Figures S1−S3 of the Supporting Information). This can lead to introduction of errors, which significantly alters the final result in determination of affinity. Through the course of our own and others research, we have learned that depending on the method of processing spectral data obtained by ratiometric measurements, we obtain significantly different K_d values.[7,8]

Received: August 19, 2013
Accepted: November 1, 2013
Published: November 1, 2013

This report presents and discusses factors in different approaches that affect proper determination of stability constants of ratiometric probes in various experimental conditions. On the basis of several chemical probes and genetically encoded sensors, we present how processing of experimental data leads to differences in determination of the affinities. Finally, we provide a simple method and appropriate formulas for data processing and determination of the K_d value for a probe with ratiometric features. Our approach also allows processing of spectral data for optical systems that have various cooperativity and stoichiometry with the same affinity toward the target molecule under different experimental conditions.

MATERIALS AND METHODS

Peptide Synthesis. Zinc ribbon peptide from TRAP protein (trp RNA-binding attenuation protein) modified at the N-terminus with dansyl chloride and C-terminal tryptophan, Dns-EVACPKCERAGEIEGTPCPACSGKGVI-LTW-NH_2 (EVA peptide) was synthesized by solid phase synthesis, as described previously.[7]

Protein Expression and Purification. Plasmid-encoding protein FRET glutamate sensor FLIPE-1μ (pRSET FLIPE intramol-1μ) was provided by Prof. Wolf Frommer (Addgene plasmid no. 13549).[5] Plasmid-encoding fluorescent ratiometric Ca(II) sensor protein GEM-GECO1 (pTorPE-GEM-GECO1) was provided by Prof. Robert Campbell (Addgene plasmid no. 32463).[3] These plasmids were used to transform chemically competent *Escherichia coli* BL21(DE3) and DH10B strains. The proteins were expressed and purified following the experimental methods in original publications.[3,5]

Equilibration of Chemical Probes and Gentically Encoded Sensors. Zincon, EVA peptide, and GEM-GECO were equilibrated in appropriate metal buffers that control unbound (free) metal ion concentration of Cu(II), Zn(II), and Ca(II), respectively. Metal buffers were prepared with 1.0 mM TPEN, CEDTA, EDTA, HEDTA, or EGTA chelator with 0−1.0 mM of appropriate metal salt. Concentrations of unbound metal ions were calculated using MinQL+ 4.6 based on published stability and protonation constants (Table S1−S3 of the Supporting Information).[9] Purified FLIPE-1μ sensor was divided into aliquots, and sodium glutamate was added to a final concentration ranging from 10 nM to 1 mM (Table S4 of the Supporting Information).[5] In every case, the concentration of unbound ligand−metal or glutamate was corrected to account for the concentration of the probe/sensor−ligand complex. For details see Tables S1−S4 of the Supporting Information.

THEORETICAL CONSIDERATIONS

Determination of the association (K_a) or dissociation (K_d) constant is usually performed by processing a set of experimental data using equilibrium equations. With dependence on the chosen methodology, the affinity of the sensor (S) to the target ligand (L) is usually calculated based on eqs 1 or 2. The binding status of the probe is usually analyzed by measurement of intensity of absorption or fluorescence (I) at a wavelength that is characterized by the largest difference between minimal and maximal intensities (I_{min}, I_{max}). It is important to choose a wavelength, at which intensity changes are proportional to binding of the target ligand, so it will not complicate the equilibrium analysis. One must also choose experimental conditions, which guarantee a proportional response of the signal to concentration. The concentration of the probe or sensor should be in the proper range so there will be no stacking or aggregation. Generally, in the case of fluorescent probes and sensors, the concentration is adjusted so the measured absorption of the solution would not exceed 0.1. Processing of the spectral data requires initial normalization of the signal intensity (I), which is accomplished by measuring borderline values: the lowest (I_{min}) and highest (I_{max}) intensity at a given wavelength, which corresponds to unbound and fully bound sensor, frequently termed the dynamic range of the sensor.

$$\frac{I - I_{min}}{I_{max} - I_{min}} = \frac{(L_t + S_t + K_d) - \sqrt{(-L_t - S_t - K_d)^2 - 4L_tS_t}}{2} \quad (1)$$

$$\frac{I - I_{min}}{I_{max} - I_{min}} = \frac{[L_u]}{K_d + [L_u]} \quad (2)$$

where I is the measured signal intensity, I_{min} is the signal intensity when the ligand is not present, I_{max} is the signal intensity when the sensor is saturated with the ligand, L_t is the total concentration of the ligand, S_t is the total concentration of the sensor, $[L_u]$ is the unbound ligand concentration, and K_d is the dissociation constant. The quadratic equation (eq 1) associates the total concentration of the ligand and sensor. Equation 2, commonly known as the one-site binding equation, requires the use of the unbound ligand concentration, which can be calculated by subtracting the concentration of the sensor−ligand complex (SL) in equilibrium from the total ligand concentration $[L_u] = L_t - SL$. If ligand binding to the sensor is dependent on other factors than affinity or the resulting complex can have a different stoichiometry, then eq 3, which includes Hill's cooperativity factor (n), is the better choice.

$$\frac{I - I_{min}}{I_{max} - I_{min}} = \frac{[L_u]^n}{K_d + [L_u]^n} \quad (3)$$

Normalization of the obtained spectral data using the lowest (I_{min}) and highest (I_{max}) intensity is very important in the estimation of $[L_u]$, especially when the sensor is used in an environment with a high background (e.g., autofluorescence). Equation 4 allows for calculation of $[L_u]$, using a sensor with known ligand affinity by normalization of the analyzed signals.

$$[L_u] = K_d\frac{I - I_{min}}{I_{max} - I} \text{ or } [L_u] = \sqrt[n]{K_d\frac{I - I_{min}}{I_{max} - I}} \quad (4)$$

Determination of the stability constant based on two different wavelengths is usually done in a similar way as presented in eqs 1−3. By dividing the signal intensity at λ_2 (long wavelength) by one at λ_1 (short wavelength), as usually can be seen in FRET-based sensors, one obtains the ratio of intensity (R) and the extent of the changes (dynamic range), which is defined by minimal and maximal ratios (R_{min}, R_{max}). Normalization of changes in ratio values leads to eqs 5 and 6, which are used for the determination of affinity from the experimental data set.

dx.doi.org/10.1021/ac402637h | *Anal. Chem.* 2013, 85, 11479−11486

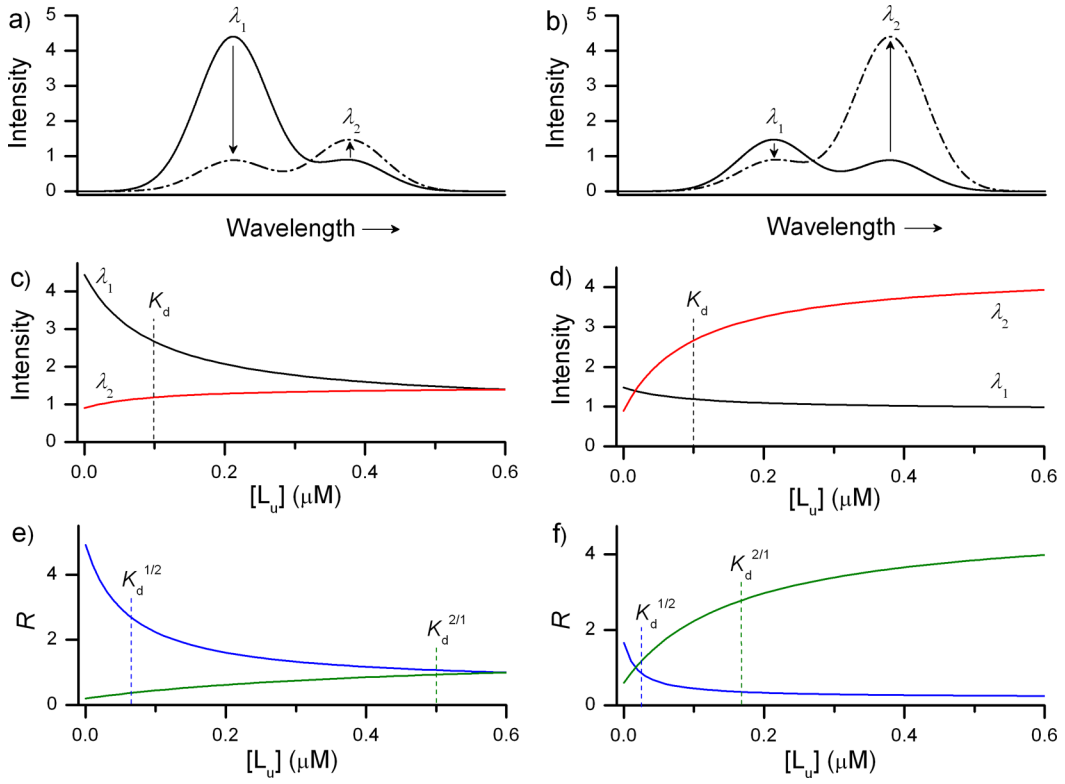

Figure 1. Simulation of spectral processing of two significantly different hypothetical ratiometric probes with K_d = 100 nM. (a and b) Intensity changes of two wavelengths upon ligand binding. Arrows show direction of the changes upon ligand binding. (c and d) Intensity changes of λ_1 and λ_2 in the function of unbound ligand $[L_u]$. Dashed black line indicates $[L_u]$ that is equal to the K_d value of the probe. (d and f) Blue and green colors represent $R_{1/2}$ and $R_{2/1}$, respectively. $K_d^{1/2 \text{ or } 2/1}$ demonstrates the values determined using either $R_{1/2}$ or $R_{2/1}$. Sensor concentration of 1 μM was assumed for calculations.

$$\frac{R - R_{min}}{R_{max} - R_{min}} = \frac{(L_t + S_t + K_d) - \sqrt{(-L_t - S_t - K_d)^2 - 4L_tS_t}}{2} \quad (5)$$

$$\frac{R - R_{min}}{R_{max} - R_{min}} = \frac{[L_u]}{K_d + [L_u]} \text{ or } \frac{R - R_{min}}{R_{max} - R_{min}} = \frac{[L_u]^n}{K_d + [L_u]^n} \quad (6)$$

Equations 5 and 6, although used very frequently for this purpose, do not calculate the dissociation constant value in terms of chemical equilibrium. This can be explained by the fact that the ratio change is not proportional to the change in saturation of the sensor (Figure 1 and Figures S2−S4 of the Supporting Information). Therefore $(R - R_{min})/(R_{max} - R)$ does not comply with $(I - I_{min})/(I_{max} - I)$ at particular wavelengths, which introduces significant errors in affinity value determination.

This report focuses on exposing this difference and showing how the results are altered when this factor is not taken into consideration. Figure 1 shows two hypothetical situations, where intensities at λ_1 and λ_2 are decreasing and increasing, respectively, upon ligand binding and the dynamic ranges differ. In this hypothetical model, the dissociation constant of the formed complex is 10^{-7} M (100 nM) and the cooperativity factor equals 1. The changes in intensities at selected wavelength bands were simulated based on eq 7 (modified Hill's equation), which is a derivative of eq 3 in terms of intensity (I).

$$I = I_b\left(\frac{x^n}{x^n + K_d^n}\right) + I_u\left(\frac{K_d^n}{x^n + K_d^n}\right) \quad (7)$$

where I_b and I_u refer to the intensity of bound and unbound sensor at the selected wavelength, respectively. The presented plot of changes in intensities at λ_1 and λ_2 as a function of free ligand (Figure 1) allows for graphical estimation of the value of K_d at the half-point of the intensity changes. These values are identical for both wavelengths. However, when intensities are divided by each other, resulting in $R_{1/2}$ ($I_{\lambda1}/I_{\lambda2}$) or $R_{2/1}$ ($I_{\lambda2}/I_{\lambda1}$) as in ratiometric sensors, then the R change half-point corresponds to a different $[L_u]$ than for a single wavelength intensity. The value of the dissociation constant will be higher or lower than the proper K_d depending on the type of ratio used ($R_{1/2}$ or $R_{2/1}$); however, there is no strict rule that binds one type of ratio with one effect (e.g., higher constant). This difference is clearly visible when we describe the changes of I or R on a logarithmic scale plot (Figure S1 and S2 of the Supporting Information). The differences between the actual K_d value and those obtained by processing the ratio data ($K_d^{1/2 \text{ or } 2/1}$) are significant. With dependence on the minimal and maximal intensities at a given wavelength, the differences between K_d will be changing (Figure S3 of the Supporting Information). In order to calculate K_d accurately, one must not consider the ratio but rather apply the direct intensities at two wavelengths simultaneously. By dividing the intensities at a given wavelength as defined in eq 7, we obtain a new

dx.doi.org/10.1021/ac402637h | Anal. Chem. 2013, 85, 11479−11486

dependence of R to I_u and I_b, without the need for considering the R_{min} and R_{max} (eqs 8 and 9).

$$R_{1/2} = \frac{I_{1b}x^n + I_{1u}K_d^n}{I_{2b}x^n + I_{2u}K_d^n} \quad (8)$$

$$R_{2/1} = \frac{I_{2b}x^n + I_{2u}K_d^n}{I_{1b}x^n + I_{1u}K_d^n} \quad (9)$$

where I_{1b} is the intensity at λ_1 of the bound sensor, I_{1u} is the intensity at λ_1 of the unbound sensor, I_{2b} is the intensity at λ_2 of the bound sensor, I_{2u} is the intensity at λ_2 of the unbound sensor, x is the concentration of unbound ligand, K_d is the dissociation constant, and n is Hill's coefficient. The new formulas also account for Hill's cooperativity factor that describes the binding of one or more ligands to the sensor with the same affinity. We want to emphasize that the above formulas bridge the classical usage of the ratio which broadens the sensing range and concentration independence with single wavelength processing that avoids K_d values shifting. Application of both equations to the data from the simulation presented in Figure 1 allows calculation of dissociation constants that are identical to the ones obtained from employing independent wavelength intensities using the assumptions $R_{1/2} = f([L_u])$ and $R_{2/1} = f([L_u])$ (Figure S4 of the Supporting Information). The point-by-point instruction on how to use our equation is given in the protocol below and in the Supporting Information.

Protocol for the determination of K_d value of optical ratiometric system:

1. Collect the intensity data (absorption or fluorescence) at two characteristic wavelengths (λ_1 and λ_2) at different ligand (analyte) concentration. Make sure that borderline points (end-points) – intensities at two wavelengths for unbound (free) and saturated sensor are precisely measured. The obtained values are I_{1u}, I_{1b}, I_{2u}, I_{2b} (intensities of unbound and saturated states read at λ_1 and λ_2, respectively).

   Note: If due to experimental nature the borderline points cannot be precisely measured then plot the unbound ligand concentration vs. intensity at λ_1. Next use Hill's equation (**Equation 7**) and fit to experimental data points. Repeat for intensities at λ_2. This way one obtains the borderline values of intensities, however, this approach may introduce some error into final calculation of dissociation constant.

2. Convert the measured intensity data to ratio by dividing the intensity at λ_1 by intensity at λ_2 ($R_{1/2}$), or other way round ($R_{2/1}$).

3. Plot the ratio data vs. concentration of unbound ligand. If the concentration of unbound ligand is significantly affected by probe/sensor-ligand complexation ligand make appropriate correction.

   Note: For high ligand to sensor affinity, we recommend plot ratio data vs. logarithmic values of unbound ligand (-log[L_u]).

4. Use the **Equation 8** (for $R_{1/2}$) or **Equation 9** (for $R_{2/1}$) to calculate the value of dissociation constant (K_d) and cooperativity factor (n). Use any software that allow to fit nonlinear curves. Set the end-point values (I_{1u}, I_{1b}, I_{2u}, I_{2b}) as fixed (constant).

   Note: If logarithmic plot is used, make sure that **Equation 8** or **9** is adjusted for this scale.

   The point by point procedure of calculation of K_d of Ca^{2+}-GEM-GECO1 with all values is presented in *Supporting information*. It should be noted that in cases where multiple ligands bind to probe or sensor the result form our equation is valid only for certain probes e.g. GEM-GECO1, but not for those displaying strong positive or negative cooperativity, with very different K_d values that should be determined separately.

RESULTS AND DISCUSSION

Rationale. Since our approach for calculating the K_d value was successfully proven on a theoretical basis and with simulated data, we decided to test it in a real experimental setup. For that purpose, we have selected four commonly used and newly designed ratiometric chemical probes and protein-based sensors that are extremely useful in many areas of research. The first, is zincon, a commonly used chromophore that binds Zn(II) and Cu(II) ions and forms zincon−Cu(II) complexes with 1:1 stoichiometry at pH 7.4 (Figure 2). The second one is a zinc ribbon (EVA peptide), with N-terminal dansyl and C-terminal tryptophan as a FRET pair, where binding of Zn(II) causes conformational changes (Figure 2).[10−12] The third one is a glutamate sensor, FLIPE-1μ, which is a good example of a common genetically encoded FRET sensor design, where two appropriate fluorescent proteins (CFP and YFP) are linked by a sensor domain ybeJ that binds the target ligand and changes its conformation, resulting in a FRET decrease (Figure 3).[5] The last one is GEM-GECO1, a genetically encoded ratiometric sensor composed of circularly permuted (cp) GPF fused with a Ca(II)-dependent domain, calmodulin (CaM), and the M13 domain of myosin. Binding of four Ca(II) results in reorganization in the structure of the fluorescent protein, which leads to significant change of fluorescence spectra (Figure 3).[3] GEM-GECO1 is considered as state-of-the-art for the measurement of Ca(II) concentration and its fluxes, which is one of the major areas of research in cell biology.[13] In the case of characterization of FLIPE-1μ and GEM-GECO1, we applied the same experimental setup as stated in the original reports and used both those authors' and our method of data processing in order to obtain the K_d value. However, in both cases, we were limited by the degree of detail in the publications (Table 1).

Experimental Results. The spectral changes of each probe and sensor upon ligand binding are presented in Figures 2 and 3, respectively. The results obtained by processing original data sets with different approaches such as one binding site model, Hill's equation, and our method are gathered in Table 1. The experimental data sets conform with the conclusions established in theoretical considerations. The calculation of K_d and n values based on single wavelengths λ_1 and λ_2 using Hill's equation yields convergent results. Our method, combining two wavelengths, no matter which ratio was used provided more coherent results than single wavelength analysis. The small difference obtained from eqs 8 and 9 (e.g., 218 and 214 nM in the case of GEM-GECO1 and 66 and 85 zM for zincon) can be attributed to the fitting process, which can give a minimally different outcome due to the least-squares methodology. However, when $R_{1/2}$ is used, despite different equations (i.e., Hill's and one binding site), the calculated K_d value is lower than the correct one and $R_{2/1}$ gives higher values. This observation is true in the case of ratiometric systems, where I_1 decreases and I_2 increases upon ligand binding (Zincon, EVA). FLIPE-1μ and GEM-GECO1 represents a system where I_1 increases and I_2 decreases upon ligand binding, which results in K_d from $R_{1/2}$ being higher and $R_{2/1}$ lower than the actual one. It is also important to note the GEM-GECO1 binds to Ca(II) with a 1:4 stoichiometry.[3] The application of the one-site binding equation here, which does not use Hill's factor, resulted in a large error. As can be seen in Table 1, our data-processing methods yielded different results than published values for FLIPE-1μ and GEM-GECO1. In both cases, the discrepancy can result from using ratio values instead of intensities, as proposed here. We also applied our data processing method on previously obtained results from FRET-based characterization of zinc hook motif, where two peptides bind one Zn(II). The final result was similar to one previously obtained, which confirms that the method presented here is also applicable for determination of K_d for complexes with stoichiometries other than 1:1.[7] Figures S5−S9 of the Supporting Information demonstrate various processing methods for data sets for all probes and sensors with appropriate fitting curves using the one binding site model, Hill's equation for both wavelengths, and

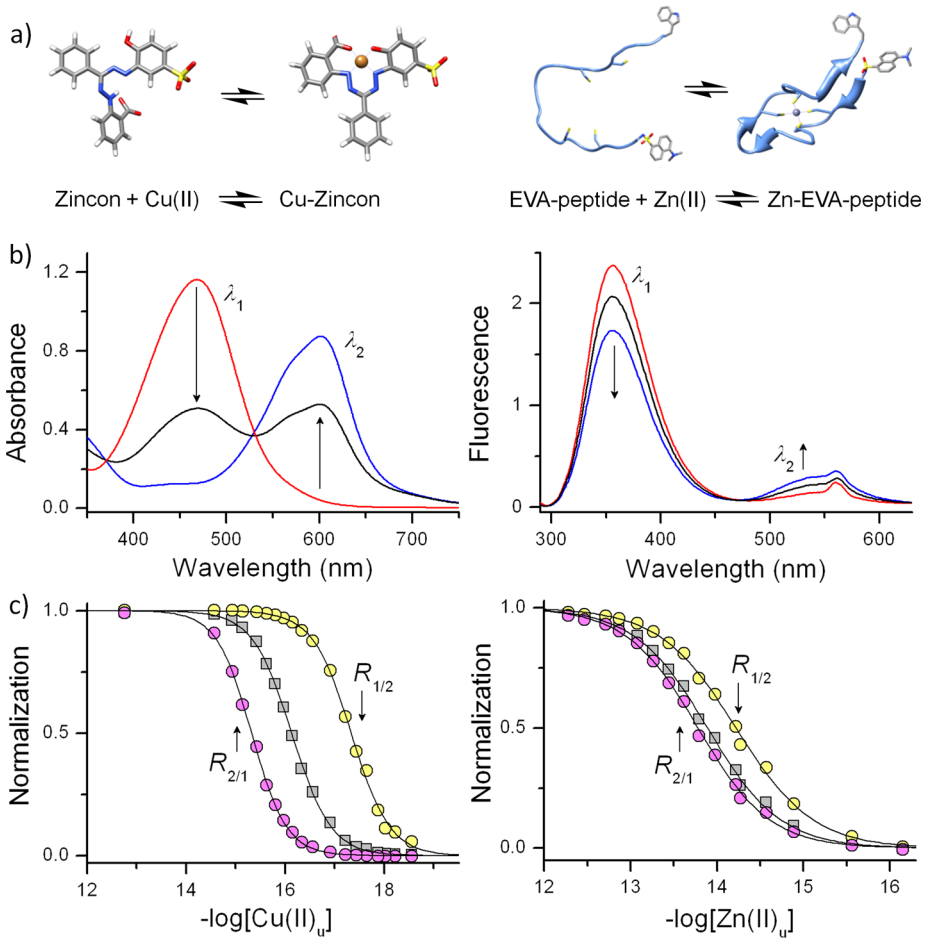

Figure 2. Complexation of Cu(II) and Zn(II) to zincon and EVA peptide. (a) Schematic representation of ligand binding. (b) Spectra changes upon metal ion binding with indication of intensity changes direction. (c) Normalized effect of ratio response or sensor saturation in the function of $-\log[Cu(II)_u]$ and $-\log[Zn(II)_u]$ values. $R_{1/2}$ and $R_{2/1}$ indicate normalized change in the $I_{\lambda 1}/I_{\lambda 2}$ and $I_{\lambda 2}/I_{\lambda 1}$ ratios, respectively. Gray squares denote actual sensor saturation, which was determined by our method (see the protocol for the detailed procedure). The concentration of zincon was 50 μM and EVA peptide 5 μM (for details about calculation of the concentration of unbound Zn(II) or Cu(II), see Tables S1 and S2 of the Supporting Information.

our approach for processing $R_{1/2}$ and $R_{2/1}$. Tables S5−S9 of the Supporting Information present all fitted values with standard errors for all used models.

The data processing method is a key point in accurate determination of K_d values. However, the spectral background or artifacts may significantly affect the accurate determination of K_d. Therefore, we decided to test whether our method can cope with artifacts commonly encountered in fluorescence measurements (Figure 4). As a model fluorophore we chose GEM-GECO1 because of the high dynamic range of fluorescence changes upon binding of Ca(II).[3] Its fluorescence data were distorted in several ways: addition of a constant baseline in the full spectrum (Figure 4a), or addition of nonconstant baselines with various slopes (Figure 4, panels b and c). We also added the fluorescence signal of the FlAsH−tetracysteine peptide (TC) complex, whose fluorescence spectra coincides with GEM-GECO1 fluorescence (Figure 4d).[14] As can be seen in Figure 4, our method gives the same value of K_d as an unmodified GEM-GECO1 spectra. The normal Hill's equation with ratiometric data input produces different results almost each time.

Methods Used for Determination of Affinity Constants. As presented above in both simulations and four individuals sensors, the direct processing of the intensity ratio of two wavelengths leads to significant differences between the calculated and actual affinity of the probes toward the ligand. The general equations for calculating K_d were presented in theoretical considerations (eqs 1−6); however, there are also several approaches which were developed in order to normalize the readings or subtract the background. The literature shows various applications of FRET for quantifying the interactions between molecules and often presents different methods of experimental data processing.

First of all, in some cases, the K_d of the ratiometric probe−ligand complex is calculated based only on a single wavelength. For example, the affinity of the AT180 antibody toward phosphorylated CDK Tau peptides was measured by tryptophan-dansyl FRET and the K_d value obtained by fitting the changes in intensity of dansyl fluorescence into the quadratic equation.[15] Although this approach gives good results, it may introduce significant errors if the concentration of the sensing molecule is not precisely estimated or fluorescence is disrupted by a number of artifacts.

The most frequently used methods are usually based on the processing of $R_{1/2}$ or $R_{2/1}$ values as dependent variables, with the second being the most popular. It was used for example to assess the K_d of a new, genetically encoded linker, ER/K, that can regulate the frequency of interaction between two

dx.doi.org/10.1021/ac402637h | Anal. Chem. 2013, 85, 11479−11486

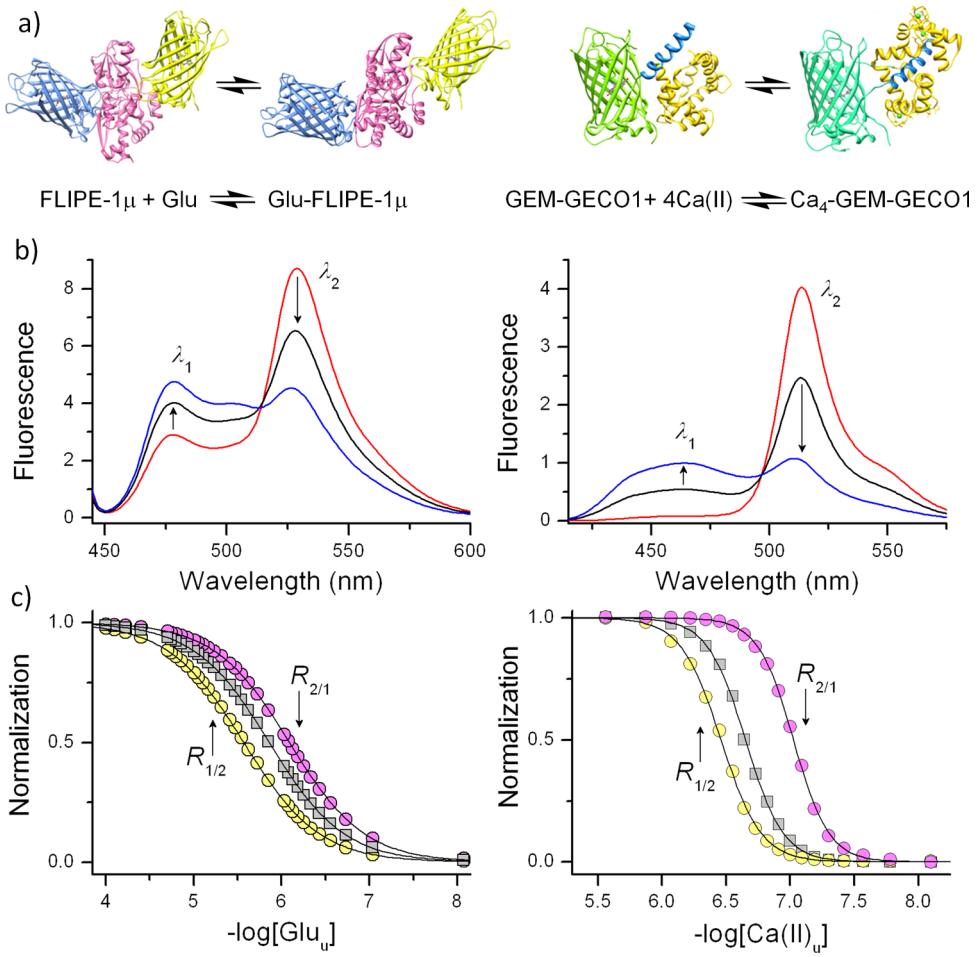

Figure 3. Binding of Glu and Ca(II) to genetically encoded sensors FLIPE-1μ and GEM-GECO1. (a) Schematic representation of ligand binding. (b) Spectra changes upon ligand binding with indication of intensity changes direction. (c) Normalized effect of ratio response or sensor saturation in the function of $-\log[\mathrm{Glu_u}]$ and $-\log[\mathrm{Ca(II)_u}]$ values. $R_{1/2}$ and $R_{2/1}$ indicate normalized changes in the $I_{\lambda1}/I_{\lambda2}$ and $I_{\lambda2}/I_{\lambda1}$ ratios, respectively. Gray squares denote actual sensor saturation, which was determined by our method (see the protocol for the detailed procedure). The concentration of FLIPE was 0.25 μM and GEM-GECO1 0.5 μM (for details about the calculation of the concentration of unbound Glu or Ca(II) see Tables S3 and S4 of the Supporting Information.

proteins.[16] Interestingly, in this experimental setup, the changes of ratio due to binding are almost linear, but despite the linear regression factor $r^2 = 0.993$, the curvature of the plot is clearly visible. In another work, the $R_{2/1}$ ratio was used in the development of methodology that identifies interacting proteins.[17] It is stated that this approach gave a lower K_d value of the interaction of the target protein pair than previously established. The value of the ratio can also be normalized, which was done during the in vitro characterization of the Na(I)−Ca(II) exchanger.[18] Ratio of $R_{2/1}$ is frequently used in order to obtain K_d by fitting the titration curves into eq 10 for the protein−ligand binding (one-site saturation binding isotherm):

$$S = \frac{R - R_{min}}{R_{max} - R_{min}} = \frac{L_t - [L_u]}{L_t} = \frac{z[L_u]}{K_d + [L_u]} \qquad (10)$$

where S is saturation (frequently named occupancy), $[L]$ is ligand concentration, $[L_u]$ is concentration of unbound ligand, L_t is total concentration of ligand, and z is the number of equal sites binding. This approach is used for example to describe the metabolite sensors developed by Frommer's group or, most recently, the glucose indicator or interaction of apigenin with heterogeneous nuclear ribonucleoprotein A2.[5,19−21] The normalized ratio change is often given in a percent scale, which is widely used in publications describing development of new protein-based Ca(II) and Cu(I) sensors.[23−26] The other method uses $\Delta R/R$ or its % of maximum ratio, where ΔR is the change of ratio and R is the baseline ratio. It was used for example in characterization of CerTN-L15 and the TNXL family Ca(II) sensors.[27,28] Despite the different methods of ratio processing, the calculated value of K_d will still be shifted in the way presented before, even though in some cases the error will be marginal. As can be seen from the analysis of differences between K_d values obtained by different processing methods, the extent of the error is variable and depends on differences in spectral changes of a given ratiometric system, so without raw data, it is difficult to determine whether the previously obtained affinity constants have significant error.

An interesting approach is presented in the work by Bozym et al., which presents a Zn(II) sensor based on carbonic anhydrase, labeled with Alexa Fluor 594, which binds dapoxyl sulfonamide via Zn(II) that constitutes a FRET pair.[22] The ratio was obtained by dividing the Alexa Fluor 594 emission intensity due to FRET from dapoxyl sulfonamide and the intensity of Alexa Fluor by direct excitation of this acceptor, which in essence normalized the signal. Here, the numerator is

dx.doi.org/10.1021/ac402637h | Anal. Chem. 2013, 85, 11479−11486

Table 1. Dissociation Constants of Ratiometric Probes and Sensors Calculated Using Various Processing Methods[a]

processing method	K_d and cooperativity coefficient factor (n)			
	Zincon (zM)	EVA peptide (fM)	FLIPE-1μ (μM)	GEM-GECO1 (nM)
λ_1 processing, Hill's equation	66 ± 3	13 ± 1	1.38 ± 0.03	228 ± 5
	(1.12 ± 0.02)	(1.07 ± 0.06)	(1.03 ± 0.01)	(2.89 ± 0.07)
λ_2 processing, Hill's equation	85 ± 2	12.6 ± 0.6	1.41 ± 0.03	215 ± 5
	(1.02 ± 0.02)	(1.02 ± 0.05)	(1.03 ± 0.01)	(2.97 ± 0.06)
$R_{1/2}$, one binding site equation	4.4 ± 0.2	6.0 ± 0.3	2.63 ± 0.06	589 ± 170
	(−)	(−)	(−)	(−)
$R_{1/2}$, Hill's equation	4.7 ± 0.2	6.0 ± 0.3	2.69 ± 0.06	347 ± 42
	(1.12 ± 0.05)	(0.98 ± 0.05)	(1.02 ± 0.01)	(2.81 ± 0.08)
$R_{2/1}$, one binding site equation	524 ± 38	17.0 ± 0.8	0.81 ± 0.02	93 ± 30
	(−)	(−)	(−)	(−)
$R_{2/1}$, Hill's equation	479 ± 11	16.6 ± 0.8	0.83 ± 0.02	93 ± 7
	(1.23 ± 0.02)	(1.05 ± 0.04)	(1.03 ± 0.01)	(3.15 ± 0.06)
$R_{1/2}$, our method	71 ± 3	12.9 ± 0.3	1.38 ± 0.03	221 ± 3
	(1.10 ± 0.03)	(1.01 ± 0.03)	(1.02 ± 0.01)	(2.74 ± 0.06)
$R_{2/1}$, our method	74 ± 4	12.9 ± 0.3	1.38 ± 0.03	215 ± 2
	(1.15 ± 0.03)	(1.04 ± 0.02)	(1.03 ± 0.01)	(3.09 ± 0.05)
ref[3,5]	–	–	1.0	340
	(−)	(−)	(n.d.)	(2.94)

[a] $R_{1/2}$, $R_{2/1}$, and n refer to intensity ratios between two intensities and Hill's coefficient, respectively.

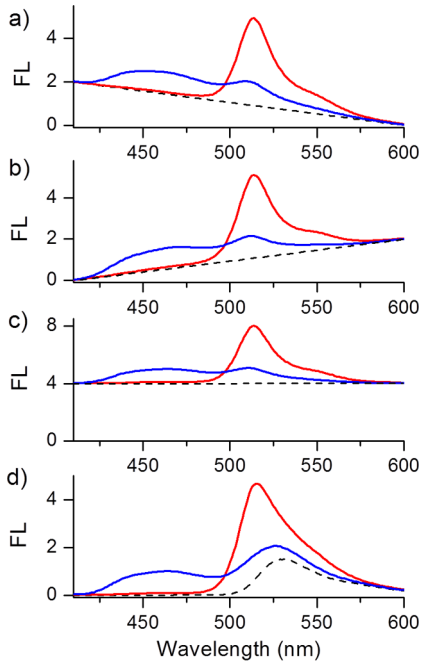

a-d	K_d (nM) - $R_{1/2}$ Hill's equation	K_d (nM) - $R_{1/2}$ Our method
a)	298 ± 4	219 ± 4
b)	295 ± 3	220 ± 3
c)	255 ± 2	222 ± 3
d)	312 ± 3	221 ± 4

Figure 4. Simulation of common artifacts (dashed lines) that accompanies fluorescence measurements and resulting K_d values calculated from ratiometric data ($R_{1/2} = I_1/I_2$) using Hill's equation or our method.

practically constant, every point is divided by the same number, which does not affect the K_d determination.

The two scenarios where optical ratiometric systems are used for determination of K_d is establishment of protein−protein or protein−ligand affinity and development of ratiometric sensors (e.g., for metal ions such as Ca(II) or Zn(II) or small molecules), which can be subsequently used in the measurement of the concentration of ligand. In the case of interacting molecules, the situation is rather simple: the value of the dissociation constant is directly used to form conclusions. However, it is more complex in the sensor area. The dissociation constant is utilized to calculate the concentration of target ligand based on the ratiometric signal. In this type of application, K_{eff} is used in most equations for calculating the concentration of target ligand.[10,29−31] K_{eff} is an effective binding constant and corresponds to the ratio change due to sensor response to various concentrations of ligand. Therefore, K_{eff} value equals the ligand concentration at which the R value is in the middle between R_{min} and R_{max} and does not directly reflect the K_d of the ligand−sensor complex. The relation between K_{eff} and K_d can be described by eq 11:

$$K_{eff} = K_d\left(\frac{S_{u2}}{S_{b2}}\right) \tag{11}$$

where S_{u2} is the value of I_2 of the unbound sensor and S_{b2} is the value of I_2 of ligand-bound sensor.[31] One should remember that because K_{eff} does not reflect the real dissociation constant, it can be used for estimation of the target molecule concentration only when the sensor shows the same dynamic range of ratio change during measurements and characterization which led to the determination of K_{eff}. This is almost never true, since most of the sensors used for in vivo measurements are characterized in vitro and often show a different dynamic range of ratio change when used in intracellular measurements.[8] Despite this fact, many authors use K_{eff} and K_d interchangeably. An interesting example here is the genetically encoded eCALWY sensor family, which was designed and applied to measure the cell free Zn(II) by the Merkx group.[4] By manipulation in the linker region between metal ion binding domains, several sensors with different affinities for Zn(II) were designed. The K_d values, which were calculated based on the citrine to cerulean protein fluorescence

dx.doi.org/10.1021/ac402637h | Anal. Chem. 2013, 85, 11479−11486

ratio ($R_{2/1}$) using the one-site binding equation (eq 6), are in fact K_{eff} values. The comparison of occupancy of different sensors in pancreatic β cells with simulations of sensor occupancy allows calculation of cell free Zn(II). However, this is only valid if the dynamic range is the same in conditions used in measurement in vivo and characterization of sensor K_d in vitro.

There are also other methods that can be used to determine the dissociation constant in an optical ratiometric based experimental setup that do not rely on fluorescence intensity or ratio. These include usage of FRET efficiency, fluorescence anisotropy, and time-resolved fluorescence measurements.[32−35]

CONCLUSIONS

In conclusion, we have developed a method of processing the data from a ratiometric optical system in order to calculate K_d, using borderline signal intensities at two wavelengths rather than R_{min} and R_{max}. The currently used methods that rely on a ratio lead to the introduction of processing errors that affects the accurate determination of K_d values. In contrast, our method copes not only with systems in different conditions and commonly observed fluorescence artifacts but also with different stoichiometries, provided that multiple ligands binds with similar affinity to the probe or sensor.

ASSOCIATED CONTENT

Supporting Information

Ready to use copy-and-paste formulas for calculation of accurate K_d using $R_{1/2}$ or $R_{2/1}$ fluorescence ratios, additional figures, tables, materials, and methods. This material is available free of charge via the Internet at http://pubs.acs.org.

AUTHOR INFORMATION

Corresponding Author

*E-mail: krezel@biotech.uni.wroc.pl.

Author Contributions

[†]A.P. and T.K. contributed equally to this work. All authors have given approval to the final version of the manuscript.

Notes

The authors declare no competing financial interest.

ACKNOWLEDGMENTS

This work was supported by the National Science Centre under Grant 2011/01/B/ST5/00830. Liberty 1 system used for peptide synthesis was founded by the Polish Foundation for Science under FOCUS Grant FG1/2010.

REFERENCES

(1) Grynkiewicz, G.; Poenie, M.; Tsien, R. Y. *J. Biol. Chem.* **1985**, *260*, 3440−3450.
(2) Sikorska, M.; Krężel, A.; Otlewski, J. *J. Inorg. Biochem.* **2012**, *115*, 28−35.
(3) Zhao, Y.; Araki, S.; Wu, J.; Teramoto, T.; Chang, Y. F.; Nakano, M.; Abdelfattah, A. S.; Fujiwara, M.; Ishihara, T.; Nagai, T.; Campbell, R. E. *Science* **2011**, *333*, 1888−1891.
(4) Vinkenborg, J. L.; Nicolson, T. J.; Bellomo, E. A.; Koay, M. S.; Rutter, G. A.; Merkx, M. *Nat. Methods* **2009**, *6*, 737−740.
(5) Deuschle, K.; Okumoto, S.; Fehr, M.; Looger, L. L.; Kozhukh, L.; Frommer, W. B. *Protein Sci.* **2005**, *14*, 2304−2314.
(6) Zhang, Y.; Xie, Q.; Robertson, J. B.; Johnson, C. H. *PLoS One* **2012**, *7*, e43072.
(7) Kochańczyk, T.; Jakimowicz, P.; Krężel, A. *Chem. Commun. (Cambidge, U.K.)* **2013**, *49*, 1312−4.
(8) Qin, Y.; Dittmer, P. J.; Park, J. G.; Jansen, K. B.; Palmer, A. E. *Proc. Natl. Acad. Sci. U.S.A.* **2011**, *108*, 7351−7356.
(9) Schecher, W. D.; McAvoy, D. C. Environmental Research Software: Hallwell, ME, 2003.
(10) Dittmer, P. J.; Miranda, J. G.; Gorski, J. A.; Palmer, A. E. *J. Biol. Chem.* **2009**, *284*, 16289−16297.
(11) Eis, P. S.; Lakowicz, J. R. *Biochemistry* **1993**, *32*, 7981−7993.
(12) Godwin, H. A.; Berg, J. M. *J. Am. Chem. Soc.* **1996**, *118*, 6514−6515.
(13) Clapham, D. E. *Cell* **2007**, *131*, 1047−1058.
(14) Pomorski, A.; Krężel, A. *ChemBioChem* **2011**, *12*, 1152−1167.
(15) Amniai, L.; Lippens, G.; Landrieu, I. *Biochem. Biophys. Res. Commun.* **2011**, *412*, 743−746.
(16) Sivaramakrishnan, S.; Spudich, J. A. *Proc. Natl. Acad. Sci. U.S.A.* **2011**, *108*, 20467−20472.
(17) You, X.; Nguyen, A. W.; Jabaiah, A.; Sheff, M. A.; Thorn, K. S.; Daugherty, P. S. *Proc. Natl. Acad. Sci. U.S.A.* **2006**, *103*, 18458−18463.
(18) Ottolia, M.; Philipson, K. D.; John, S. *Biophys. J.* **2004**, *87*, 899−906.
(19) Fehr, M.; Frommer, W. B.; Lalonde, S. *Proc. Natl. Acad. Sci. U.S.A.* **2002**, *99*, 9846−9851.
(20) Jin, S.; Veetil, J. V.; Garrett, J. R.; Ye, K. *Biosens. Bioelectron.* **2011**, *26*, 3427−3431.
(21) Arango, D.; Morohashi, K.; Yilmaz, A.; Kuramochi, K.; Parihar, A.; Brahimaj, B.; Grotewold, E.; Doseff, A. I. *Proc. Natl. Acad. Sci. U.S.A.* **2013**, *110*, E2153−E2162.
(22) Bozym, R. A.; Thompson, R. B.; Stoddard, A. K.; Fierke, C. A. *ACS Chem. Biol.* **2006**, *1*, 103−111.
(23) Nagai, T.; Yamada, S.; Tominaga, T.; Ichikawa, M.; Miyawaki, A. *Proc. Natl. Acad. Sci. U.S.A.* **2004**, *101*, 10554−10559.
(24) Truong, K.; Sawano, A.; Mizuno, H.; Hama, H.; Tong, K. I.; Mal, T. K.; Miyawaki, A.; Ikura, M. *Nat. Struct. Biol.* **2001**, *8*, 1069−1073.
(25) Wegner, S. V.; Arslan, H.; Sunbul, M.; Yin, J.; He, C. *J. Am. Chem. Soc.* **2010**, *132*, 2567−2569.
(26) Wegner, S. V.; Sun, F.; Hernandez, N.; He, C. *Chem. Commun. (Cambridge, U.K.)* **2011**, *47*, 2571−2573.
(27) Mank, M.; Reiff, D. F.; Heim, N.; Friedrich, M. W.; Borst, A.; Griesbeck, O. *Biophys. J.* **2006**, *90*, 1790−1796.
(28) Heim, N.; Garaschuk, O.; Friedrich, M. W.; Mank, M.; Milos, R. I.; Kovalchuk, Y.; Konnerth, A.; Griesbeck, O. *Nat. Methods* **2007**, *4*, 127−129.
(29) Miyawaki, A.; Llopis, J.; Heim, R.; McCaffery, J. M.; Adams, J. A.; Ikura, M.; Tsien, R. Y. *Nature* **1997**, *388*, 882−887.
(30) Miyawaki, A.; Griesbeck, O.; Heim, R.; Tsien, R. Y. *Proc. Natl. Acad. Sci. U.S.A.* **1999**, *96*, 2135−2140.
(31) Helmchen, F. *Cold Spring Harbor Protocols* **2011**, *2011*, 923−930.
(32) Lichten, C. A.; Swain, P. S. *BMC Biophys.* **2011**, *4*, 10.
(33) Fiegland, L. R.; Garst, A. D.; Batey, R. T.; Nesbitt, D. J. *Biochemistry* **2012**, *51*, 9223−9233.
(34) Yu, P.; Pettigrew, D. W. *Biochemistry* **2003**, *42*, 4243−4252.
(35) Benjamin, H.; Rumen, I.; Silke, A.; Reinhard, K.; Gregor, J. *J. Fluoresc.* **2011**, *21*, 2143−2153.